Stopping force on point charges in cylindrical wires

A. A. Aligia, J. L. Gervasoni, and N. R. Arista
Centro Atómico Bariloche and Instituto Balseiro, Comisión Nacional de Energía Atómica, 8400 S.C. de Bariloche, Argentina
(Received 4 June 2004; revised manuscript received 19 August 2004; published 22 December 2004)

We calculate the stopping force of charged particles traveling parallel to the axis of a cylindrical wire due to collective excitations. We used a recently developed formalism, based on a semiclassical dielectric function and the interaction of the particle with bulk and surface collective modes. The equivalence of both classical and quantum-mechanical results is demonstrated. The different contributions to the stopping force are discussed in detail on the basis of analytical and numerical results. We propose a simple way to handle the divergences due to excitations of some bulk modes.

DOI: 10.1103/PhysRevB.70.235331 PACS number(s): 73.63.−b, 73.20.Mf, 71.45.Gm, 72.30.+q

I. INTRODUCTION

The subject of the interaction of charged particles with small systems, with a typical length scale of several nm, has attracted much interest recently. For example, it has been shown that carbon nanotubes can steer charged particle beams.[1–4] In addition, studies of electron-energy-loss spectroscopy[5] and plasmon excitations[6,7] have been carried out. The excitation of bulk and surface plasmons by external charges is one of the main sources of the stopping force for a wide range of energies and is a very active field of research by its own. In addition to cylindrical cavities and wires described below, plasmon excitations were also studied in quasi-one-dimensional quantum wires.[8,9]

There are several previous studies of electron spectroscopy of nanosystems based on classical descriptions of the medium, dealing, in particular, with semiclassical dielectric models.[10–13] The transport and stopping force of charged particles inside cylindrical cavities has been studied using the dielectric response formalism[14–18] and linearized hydrodynamic theory.[19] These studies are relevant for single wall nanotubes. In multiwall nanotubes a different physics is expected due to larger screening.[20,21] Multiwall carbon nanotubes of ~6.5 nm external diameter and ~2.2 nm internal diameter were produced using arc-discharge evaporation.[22] The outer diameter can reach 30 nm.[23] Recently manganite-oxide-based nanotubes[24] and nanowires of diameter between 50 and 100 nm[25] were synthesized.

Two of us have studied plasmon excitations in cylindrical wires by external charged particles using the dielectric formalism,[26] both classically and quantum mechanically. It was shown that both approaches give identical results for the contribution of each surface mode to the stopping power. For bulk modes, some numerical results suggest that classical and quantum results coincide within numerical errors, but a rigorous proof is lacking. This proof is important for conceptual insight and also for practical calculations, since the classical expression is much simpler than the quantum one. Previously, the equivalence between classical and the quantum descriptions has been studied by Lucas *et al.* for the case of foil excitations,[27] by Ferrell and Ritchie for the case of spherical targets,[28] by Denton *et al.* for plane surfaces,[29] and by Arista and Fuentes for cylindrical cavities.[17] However, in most cases, no rigorous proof of the equivalence was given.

In this work we calculate the contributions of surface and bulk plasmons to the stopping force of a charged particle traveling inside a cylindrical massive wire and parallel to the axis of it. A local approximation for the dielectric response will be considered following the lines of previous approaches,[13–17,26] and the calculations will be restricted to swift charged particles ($v \gg v_0$, where $v_0 = 2.18 \times 10^8$ cm/s is the Bohr velocity). The former approximation means that the effects of spatial dispersion will be neglected. These effects become relevant for interactions taking place at close distances from the surface (typically, distances of the order of 1 Å). The justification of these two approximations comes from the fact that the excitations produced by a moving particle with velocity v satisfy the condition $\omega \sim kv$ (ω being the frequency of the excitation and k the wave vector). Hence, assuming typical surface plasma frequencies $\omega \sim \omega_s \sim 10$ eV/$\hbar$, the wavelengths of these excitations become of the order of $\lambda = 2\pi/k \sim 2\pi v/\omega_s$, which for velocities in the nonrelativistic range $v/v_0 \sim 10-30$, yields values in the range of several hundred Å. In these conditions, the use of a local dielectric function is a convenient approximation.

In the bulk case, a quantitative calculation requires the introduction of a short distance cutoff and also a cutoff in the angular momentum of the modes to avoid divergences. We justify these cutoffs by physical considerations. Fortunately, the results are weakly dependent on them. We also present a rigorous proof of the equivalence between classical and quantum results.

The paper is organized as follows. In Sec. II, we present the relevant expressions that follow from the dielectric formalism[26] and discuss the limitations of the approach and the need to introduce cutoffs. The mathematical details of the proof of the equivalence between classical and quantum results for the bulk part of the stopping force are left to the Appendix. Section III contains the results for the stopping force. Section IV is a summary and discussion.

II. FORMALISM AND RELEVANT EQUATIONS

A. Surface modes

The electrostatic surface modes are obtained from the Laplace equation $\nabla^2\phi = 0$ matching the solutions inside and outside the wire.[26,13] In cylindrical coordinates, for a given angular momentum projection m, the solution takes the form

(a) for $\rho < a$

$$\phi_{sm}^{(1)}(\rho,\varphi,z) = A_m e^{i(kz+m\varphi)} I_m(k\rho) e^{-i\omega t}, \tag{1}$$

(b) for $\rho > a$

$$\phi^{(2)}_{sm}(\rho,\varphi,z) = B_m e^{i(kz+m\varphi)} K_m(k\rho) e^{-i\omega t}, \tag{2}$$

where a is the radius of the cylinder, k is a wave vector along z (the wire direction), and $I_m(x)$, $K_m(x)$ are Bessel functions. From the matching conditions, and using a simple approximation for the dielectric constant

$$\varepsilon(\omega) = 1 - \omega_p^2/\omega(\omega + i\eta), \ \eta \to 0^+, \tag{3}$$

where ω_p is the plasma frequency, the dispersion relation of the surface modes is obtained

$$\omega^2_{sk_m} = \omega_p^2 x I'_m(x) K_m(x), \tag{4}$$

where the prime denotes the derivative with respect to $x = k_m a$. The subscript m in the wave vector is to remind us that when a particle with velocity v travels along the wire, the modes with wave vector $k_m(v) = \omega_{sk_m}/v$ are excited.

The classical stopping force is calculated from the effect of the induced reaction of the medium on the moving particle. The corresponding quantum result is obtained expressing the total energy of the system and the electrostatic potential in terms of creation and annihilation operators for plasmon modes, and solving the evolution of the system due to the particle-field interaction.[26] It turns out that the classical and quantum results coincide and the stopping power of a particle traveling inside the wire at a distance ρ_0 from the axis, due to surface plasmons is

$$F_s = -F_0 \sum_m f^s_m, \tag{5}$$

$$f^s_m = k_m a K_m(k_m a) |K'_m(k_m a)| [I_m(k_m \rho_0)]^2, \tag{6}$$

$$F_0 = \left(\frac{Ze\omega_p}{v}\right)^2, \tag{7}$$

where Ze is the charge of the particle. For fixed velocity v, ω_{sk_m} should be obtained for each m solving Eq. (4). Calling $k = \omega_p/v$, from now on, and $r_m = k_m/k = \omega_{sk_m}/\omega_p$, this equation can be cast in the form

$$r_m = ka I'_m(kar_m) K_m(kar_m). \tag{8}$$

B. Bulk modes

The bulk plasma modes correspond to oscillations of the electron density n vibrating with the plasma frequency ω_p and satisfying the Poisson equation $\nabla^2 \phi_b(\rho,z,\varphi) = -4\pi e n(\rho,z,\varphi)$. The solution of this equation, for the modes with angular momentum projection m leads to

$$\phi_{bm}(\rho,z,\varphi) = \frac{4\pi e}{k^2+q^2} n_b(\rho,z,\varphi) \sim J_m(q\rho) e^{i(kz+m\varphi)} e^{-i\omega_p t}. \tag{9}$$

The boundary condition $\phi_{bm}|_{\rho=a} = 0$, yields $J_m(qa) = 0$, implying that the transverse momentum q is quantized and the allowed values are $q_{m,n} = x_{m,n}/a$, where $x_{m,n}$ $(n = 1, 2, \ldots)$ are the zeros of the Bessel function J_m. Proceeding in a similar way as before, the bulk contribution to the stopping power turns out to be[26]

$$F_b = -F_0 \sum_m f^b_m(ka, k\rho_0), \tag{10}$$

where the function $f^b_m(x,y)$ has a different expression in the classical and quantum cases:

$$f^{\rm cl}_m(x,y) = I^2_m(y)\left(\frac{K_m(y)}{I_m(y)} - \frac{K_m(x)}{I_m(x)}\right), \tag{11}$$

$$f^{\rm qm}_m(x,y) = \sum_{n=0}^{\infty} \left[\frac{2}{(x^2_{m,n}+x^2)} \frac{J^2_m(x_{m,n}y/x)}{J^2_{m+1}(x_{m,n})}\right]. \tag{12}$$

We have found that both expressions are equivalent. The proof is lengthy and requires the use of Cauchy theorem of complex variables and several tricks. It is in the Appendix. From now on, we use Eq. (11) for explicit evaluation.

C. Analysis of divergences from bulk modes

When using Eq. (10) two problems appear which can lead to a divergent (unphysical) result for the stopping force. First, if the particle travels along the axis of the wire ($\rho_0 = 0$), f^b_0 diverges logarithmically due to the corresponding divergence of $K_0(y)$ near the origin.[30] Second, the sum over angular momentum projections m ($\Sigma_m f^b_m, m = -\infty$ to $+\infty$) also diverges logarithmically for any value of ρ_0. Both shortcomings have the same origin: at wave vector larger than a critical one k_c (or distances smaller than k_c^{-1}), the expression (3) for the dielectric constant ceases to be valid and particle-hole excitations lead to additional screening and overdamping of the plasma modes.[31]

Concerning the first problem, an analysis based on the electric field when the charge distribution is replaced by a point charge suggests replacing ρ_0 by $(\rho_0^2 + k_c^{-2})^{1/2}$ in the argument of $K_0(k\rho_0)$. We have simply avoided the calculation of $K_0(k\rho_0)$ for very small ρ_0.

On the other hand, the modes for large $|m|$ do not exist and we must also introduce a cutoff. A reasonable criterion is that the azimuthal wave length at a distance $a/2$ from the center should be larger than k_c^{-1} or, in other words,

$$|m| < \pi a k_c. \tag{13}$$

In the next section we show that the results are weakly dependent on this cutoff.

III. RESULTS

In order to discuss the order of magnitude of the different relevant quantities, we take the case of carbon systems, with four valence electrons per C atom. Using the density of graphite, this gives an electron density $n = 0.451/\text{Å}^3$, suggesting $k_c = 0.77\ \text{Å}^{-1}$ and $\hbar\omega_p = 2\hbar e(\pi n/m)^{1/2} \simeq 25$ eV. The condition $k = \omega_p/v < k_c$ implies for the velocity $v > 4.9 \times 10^6$ m/s. Also, $v < c = 3 \times 10^8$ m/s implies $k > 0.013\ \text{Å}^{-1}$. A typical external radius of a multiwall nano-

tube is ~30 Å or higher.[22,23] Thus, from Eq. (13), the sum over m in the expression of F_b [Eq. (10)] should be cut off at $|m|=m_{\max}\sim 100$.

The expressions (6) and (11) entering the stopping force can be simplified considerably for $ka\ll 1$ (implying also $k\rho_0\ll 1$), taking the leading behavior of the Bessel functions for small arguments.[30] Using this we obtain for the solution of Eqs. (8):

$$r_0=\frac{2}{ka}\exp\left(-\frac{2}{(ka)^2}\right),$$

$$r_m=1/\sqrt{2},\ |m|>0. \tag{14}$$

As a consequence of either a factor r_0 or extra powers of ka, the surface f_m^s is negligible in comparison with the bulk contributions for $ka\ll 1$, except for $\rho_0=a$, where f_m^b vanishes. For the dominant bulk modes one obtains

$$f_0^b\cong \ln(a/\rho_0),$$

$$f_m^b\cong\frac{1}{2m}\left[1-\left(\frac{\rho_0}{a}\right)^2\right],\ |m|>0. \tag{15}$$

As discussed in the previous section, f_0^b has a divergence for $\rho_0\to 0$, but our results are not valid for $\rho_0<k_c^{-1}$. For $|m|>0$, f_m^b is smooth and falls rather abruptly to zero at $\rho_0=a$.

For $ka\gg 1$, $r_m=1/\sqrt{2}$ for all m. If $k\rho_0\ll 1$ and $ka\gg 1$, the bulk modes still dominate and

$$f_0^b\cong -\ln(k\rho_0/2),$$

$$f_m^b\cong\frac{1}{2m},\ |m|>0. \tag{16}$$

For $k\rho_0\gg 1$ (implying $ka\gg 1$), and not too large $|m|\ll 8k\rho_0$, one obtains independently of m

$$f_m^b\cong\frac{1}{2k\rho_0}\{1-\exp[-2k(a-\rho_0)]\}, \tag{17}$$

while the corresponding amplitude due to surface modes is

$$f_m^s\cong\frac{1}{2\sqrt{2}k\rho_0}\exp[-\sqrt{2}k(a-\rho_0)]. \tag{18}$$

Note that while f_m^b is nearly constant and falls exponentially to zero for $\rho_0\sim a$, the surface part has an exponential increase in that region, but with a smaller exponent. This is reminiscent of the Begrenzung effect for particles traveling perpendicular to a plane surface, in which the decrease of the stopping force due to bulk plasmons near the surface is exactly compensated by the corresponding increase of the contribution of surface plasmons.[32]

To study the contribution of modes with large $|m|$ for $ka\gg 1$, or the intermediate case $ka\sim 1$, one has to do numerical calculations. In Fig. 1 we show the results of numerical evaluation of Eqs. (5)–(7), (10), and (11) for $ka=1$ and $ka=10$. We solved Eq. (8) for $m=0$. For the remaining modes we took $r_m=1/\sqrt{2}$, which is an excellent approximation.[26] The cutoff in ρ_0 was set at $0.01a$ and that of $|m|$ at $m_{\max}=100$. We also show results for $m_{\max}=50$ and $m_{\max}=200$. The changes are rather small, with a moderate increase of the bulk contribution F_b with $m_{\max}$.

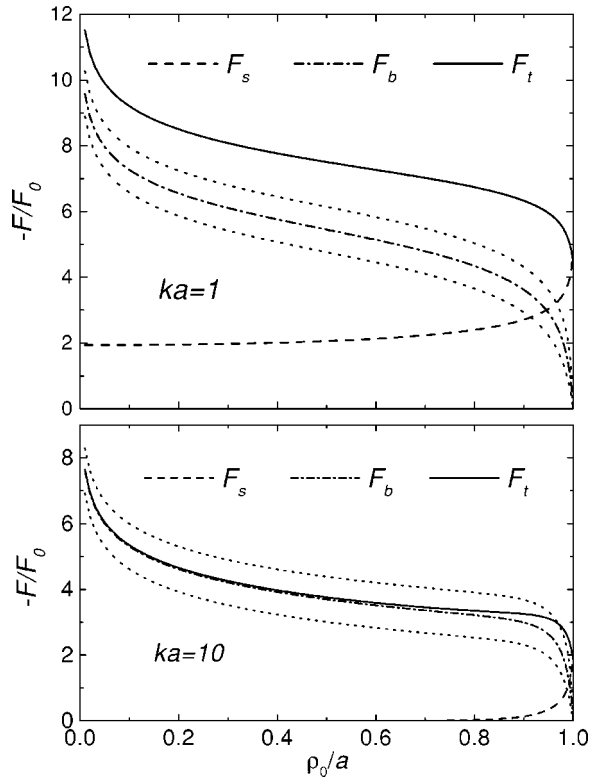

FIG. 1. Total stopping force (F_t) and surface and bulk contributions (F_s,F_b) as a function of the distance from the axis of the cylinder for two different values of $k=\omega_p/v$. For F_b the modes with $|m|\leqslant m_{\max}=100$ have been summed. The results for $m_{\max}=50$ and $m_{\max}=200$ are shown with dotted lines.

As suggested by the limiting behaviors discussed above, the bulk contribution is the dominant part of the stopping force except for the case of the particle traveling very near the surface ($\rho_0\simeq a$). However, in the intermediate region $ka\sim 1$, the surface contribution is important even for $\rho_0=0$. This is due to the excitation of the uniform surface mode $m=0$, which leads to a sizeable f_0^s when $ka\sim 1$. Instead, for $ka\ll 1$, f_0^s is negligible due to the exponentially small factor $k_0=kr_0\sim\exp[-2/(ka)^2]$ [see Eqs. (6) and (14)], while for $ka\gg 1$, $k_0=k/\sqrt{2}$, but $K_0(k_0a)\sim\exp(-k_0a)$ leading also to a negligible contribution. The qualitative behavior of f_m^b for $ka=1$ is similar to that for $ka\ll 1$ explained above.

For $ka=10$, both F_b and F_s are reduced in comparison with the case $ka\sim 1$. For $ka=10$, the slope of the total stopping power F_t vs ρ_0 is dominated by the bulk contribution of the uniform modes f_0^b. The remaining contributions are flat except for $\rho_0\simeq a$, where the behavior of $F_b(\rho_0)$ and $F_s(\rho_0)$ resemble the exponential dependences discussed above for $k\rho_0\gg 1$.

We note that in an infinite (nonbounded) medium, the stopping force is[31] $F_\infty=-F_0\ln(k_cv/\omega_p)=-F_0\ln(k_c/k)$. Using $k_c=0.77$ Å^{-1} and $a=30$ Å, this gives $F_\infty=-3.66F_0$ for $ka=1$ and $F_\infty=-1.36F_0$ for $ka=10$, which can be directly compared with the values plotted in Fig. 1.

IV. SUMMARY AND DISCUSSION

Using a dielectric formalism developed previously,[26] we have demonstrated the equivalence of the quantum and classical expressions of the stopping force, due to excitation of bulk plasmons. The corresponding result for surface plasmons was shown before.[26] Therefore, our result completes the equivalence of classical and quantum formulations, which is important for the consistency of the approach and allows us to use the simpler classical expressions for the actual computation of the stopping force.

We have analyzed the limitations of the approach and the need to introduce a high momentum (low distance) cutoff in the dielectric constant for application of the formalism to real systems. We discussed the general aspect of the stopping force in several limiting cases and calculated it numerically in complementary cases, providing a general guide to the expected order of magnitude of the stopping force due to collective excitations.

For the application of the theory to multiwall nanotubes, the effect of a finite inner diameter should be considered. However, the present results suggest that the stopping force would change significantly only very near both surfaces, while in the other more general case, the order of magnitude of the stopping force can be inferred from our results. We stress that our results are not valid at distances from the boundaries less than the short distance cutoff k_c^{-1}. Another limitation is that we have not considered the effects of a finite imaginary part η in the dielectric constant which could be important for large $|m|$. In addition, for carbon nanotubes, the anisotropy of the dielectric function is important.[33] This is not the case for manganite nanowires,[25] since the basic structure is that of a cubic perovskite.

An improvement of our theory requires a more elaborate calculation of the dielectric constant, for example, using the random-phase approximation.[8,9] However, this formalism leads to a coupling of all modes with the same angular momentum projection m and in practice it can be used when only a few number of modes is important.

ACKNOWLEDGMENTS

This work was supported in part by CONICET and ANPCYT of Argentina (Grant No. PICT03-03579).

APPENDIX: EQUIVALENCE OF CLASSICAL AND QUANTUM RESULTS FOR THE BULK STOPPING FORCE

In this appendix we show the equivalence of the classical and quantum expressions for the contribution of each angular momentum projection m to the bulk stopping force F_b [see Eq. (10)]. This reduces to show the equivalence of the functions $f_m^{\mathrm{cl}}(x,y)$ and $f_m^{\mathrm{qm}}(x,y)$ defined by Eqs. (11) and (12) for $y \leqslant x$.

We start considering the following function of the complex variable z:

$$G_l(z) = \frac{1}{(z^2+x^2)} \frac{J_m^2(zy/x)}{J_l(z)J_{l+1}(z)}. \tag{A1}$$

$G_l(z)$ is analytic except eventually at $z=0$, where it behaves as $z^{2(m-l)-1}$ (Ref. 30), at the simple poles at $z=\pm ix$ and at an infinite number of simple poles given by the zeros $x_{i,n}$ of the Bessel functions $J_i(z)$ of the denominator. In addition, for $y \leqslant x$, $G_l(z)$ decays for $z \to \infty$ as $1/z^2$ or faster. Then, its integral over a circular closed circuit $z=\exp(i\varphi)R$ with $R \to \infty$ should vanish. Using Cauchy theorem this integral gives a relation between the residues at the different poles:

$$0 = \frac{1}{2\pi i} \oint G_l(z) = \sum_j \mathrm{Res}(z_j), \tag{A2}$$

where the sum runs over all poles z_j of $G_l(z)$ and $\mathrm{Res}(z_j)$ is the residue at that pole. Using properties of the Bessel functions[30] such as $J_m(-z)=(-1)^m J_m(z)$,

$$J'_m(z) = J_{m-1}(z) - \frac{m}{2} J_m(z) = -J_{m+1}(z) + \frac{m}{2} J_m(z) \tag{A3}$$

and some algebra, Eq. (A2) can be written in the form

$$B_l = A_l + B_{l+1} + R_l, \tag{A4}$$

where R_l is the residue at $z=0$ and

$$A_l = \frac{1}{ix} \frac{J_m^2(iy)}{J_l(ix)J_{l+1}(ix)}, \tag{A5}$$

$$B_l = \sum_{n=1}^{\infty} \left[\frac{2}{(x^2+x_{l,n}^2)} \frac{J_m^2(x_{l,n}y/x)}{J_{l+1}^2(x_{l,n})} \right]. \tag{A6}$$

Iterating Eq. (A4) we obtain

$$f_m^{\mathrm{qm}}(x,y) = B_m = B_{L+1} + \sum_{l=m}^{L} [A_l + R_l], \tag{A7}$$

where L is a very large number that we shall make tend to ∞. In this limit, using asymptotic expressions for J_L and $x_{L,n}$ (Ref. 30) [$x_{L,n} \sim L+2n$, $J'_L(x_{L,n}) \sim L^{-2/3}$] one can see that $B_{L+1} \to 0$, and we suppress it in the following expressions.

Up to now we have simply replaced the series Eq. (12) by another one. However, we show below that the derivative of the second member of Eq. (A7) with respect to x can be summed. Using Eq. (A3) we can prove the relation

$$\frac{\partial}{\partial x}\left(\frac{A_l}{J_m^2(iy)} \right) = \frac{1}{x}\left(\frac{1}{J_l^2(ix)} - \frac{1}{J_{l+1}^2(ix)} \right), \tag{A8}$$

and by replacing in Eq. (A7),

$$\frac{\partial}{\partial x} f_m^{\mathrm{qm}} = \frac{J_m^2(iy)}{xJ_m^2(ix)} - \frac{J_m^2(iy)}{xJ_{L+1}^2(ix)} + \frac{\partial}{\partial x} \sum_{l=0}^{L} R_l. \tag{A9}$$

For simplicity in the third term of the second member we added the sum from $l=0$ to $m-1$, since $R_l=0$ for $l<m$. We can evaluate this term for $x \neq 0$, making the change of variable $z=xz'$ and integrating over a very small circular closed circuit $z'=\exp(i\varphi)R$ with $R \to 0$:

$$2i\pi R_l = \int_\circ G_l(z)dz = \int_\circ G_l(xz')xdz$$

$$= \int_\circ (dz')\frac{J_m^2(z'y)}{(z'^2+1)}\frac{1}{x}\frac{1}{J_l(xz')J_{l+1}(yz')}. \quad \text{(A10)}$$

A similar analysis that led to Eq. (A8) gives

$$\frac{\partial}{\partial x}\left(\frac{1}{xJ_l(xz')J_{l+1}(xz')}\right) = \frac{z'}{x}\left(\frac{1}{J_l^2(xz')} - \frac{1}{J_{l+1}^2(xz')}\right). \quad \text{(A11)}$$

Then

$$2i\pi\frac{\partial}{\partial x}\sum_{l=0}^{L} R_l = \int_\circ (dz')\frac{z'J_m^2(z'y)}{x(z'^2+1)}\left[\frac{1}{J_0^2(xz')} - \frac{1}{J_{L+1}^2(xz')}\right]. \quad \text{(A12)}$$

The contribution of $1/J_0^2(xz')$ vanishes because $J_0(z)$ is regular at $z=0$. The remaining integral can be evaluated proceeding in a similar way as Eq. (A2): the closed integral over a large circular circuit vanishes. Then, the contribution of the pole at $z'=0$ should cancel those at $z'=\pm i$ and those coming from the zeros of $J_{L+1}(xz')$ at $z'=x_{L+1,n}/x$. The contribution of the latter is negligible for large enough L using the corresponding asymptotic expressions[30] [$x_{L+1,n}\sim L+2n$, $J_L'(x_{L,n})\sim L^{-2/3}$, $J_m^2(x_{L+1,n}y/x)\sim x_{L+1,n}^{-1}$]. Calculating the remaining contributions at $z'=\pm i$ one has

$$\lim_{L\to\infty}\frac{\partial}{\partial x}\sum_{l=0}^{L} R_l = \frac{J_m^2(iy)}{xJ_{L+1}^2(ix)}. \quad \text{(A13)}$$

Replacing this in Eq. (A9), taking the limit $L\to\infty$, and using $I_\nu(x)=(-i)^\nu J_\nu(ix)$[30] one obtains

$$\frac{\partial f_m^{\mathrm{qm}}}{\partial x} = \frac{1}{x}\left[\frac{I_m(y)}{I_m(x)}\right]^2. \quad \text{(A14)}$$

Deriving Eq. (11) one gets

$$\frac{\partial f_m^{\mathrm{cl}}}{\partial x} = -\frac{I_m^2(y)}{I_m^2(x)}[K_m'(x)I_m(x) - K_m(x)I_m'(x)]. \quad \text{(A15)}$$

The expression between brackets is the wronskian $W(K_m,I_m)=1/x$.[30] Therefore, from the last two expressions

$$\frac{\partial}{\partial x}f_m^{\mathrm{qm}}(x,y) = \frac{\partial}{\partial x}f_m^{\mathrm{cl}}(x,y). \quad \text{(A16)}$$

Since obviously $f_m^{\mathrm{qm}}(y,y)=f_m^{\mathrm{cl}}(y,y)=0$, we obtain the required result

$$f_m^{\mathrm{qm}}(x,y) = f_m^{\mathrm{cl}}(x,y). \quad \text{(A17)}$$

[1] N. K. Zhevago and V. I. Glebov, Phys. Lett. A **310**, 301 (2003).
[2] S. Bellucci, V. M. Biryukov, Yu. A. Chesnokov, V. Guidi, and W. Scandale, Nucl. Instrum. Methods Phys. Res. B **202**, 236 (2003).
[3] G. V. Dedkov, Nucl. Instrum. Methods Phys. Res. B **143**, 584 (1998).
[4] L. A. Gevorgian, K. A. Ispirian, and R. K. Ispirian, Nucl. Instrum. Methods Phys. Res. B **145**, 155 (1998).
[5] V. P. Dravid, X. Lin, Y. Wang, X. K. Wang, A. Yee, J. B. Ketterson, and R. P. H. Chang, Science **259**, 1601 (1993).
[6] P. M. Ajayan, S. Iijima, and T. Ichihashi, Phys. Rev. B **47**, 6859 (1993).
[7] L. A. Bursill, P. A. Stadelmann, J. L. Peng, and S. Prawer, Phys. Rev. B **49**, 2882 (1994).
[8] Q. P. Li and S. Das Sarma, Phys. Rev. B **43**, 11768 (1991).
[9] F. A. Reboredo and C. R. Proetto, Phys. Rev. B **50**, 15174 (1994).
[10] Z. L. Wang, Micron **27**, 265 (1996).
[11] S. S. Martinos and E. N. Economou, Phys. Rev. B **24**, 6908 (1981).
[12] M. Schmeits, Solid State Commun. **67**, 169 (1988).
[13] A. Rivacoba, P. Apell, and N. Zabala, Nucl. Instrum. Methods Phys. Res. B **96**, 465 (1995).
[14] Y. T. Chu, R. J. Warmack, R. H. Ritchie, J. W. Little, R. S. Becker, and T. L. Ferrel, Part. Accel. **16**, 13 (1984).
[15] C. A. Walsh, Philos. Mag. A **59**, 227 (1989).
[16] N. Zabala, A. Rivacoba, and P. M. Echenique, Surf. Sci. **209**, 465 (1989).
[17] N. R. Arista and M. A. Fuentes, Phys. Rev. B **63**, 165401 (2001).
[18] N. R. Arista, Phys. Rev. A **64**, 032901 (2001).
[19] Y.-N. Wang and Z. L. Mišković, Phys. Rev. A **69**, 022901 (2004).
[20] F. Léonard and J. Tersoff, Phys. Rev. Lett. **83**, 5174 (1999); A. A. Odintsov, *ibid.* **85**, 150 (2000).
[21] G. C. Liang, A. W. Ghosh, M. Paulsson, and S. Datta, Phys. Rev. B **69**, 115302 (2004).
[22] S. Iijima, Nature (London) **354**, 56 (1991).
[23] P. J. F. Harris, *Carbon Nanotubes and Related Structures, New Materials for the 21st Century* (Cambridge University Press, Cambridge, 1999).
[24] P. Levy, G. Leyva, H. Troiani, and R. D. Sánchez, Appl. Phys. Lett. **83**, 5247 (2003).
[25] J. Curiale, R. D. Sánchez, H. E. Troiani, H. Pastoriza, P. Levy, and A. G. Leyva, Physica B **354**, 98 (2004).
[26] J. L. Gervasoni and N. R. Arista, Phys. Rev. B **68**, 235302 (2003).
[27] A. A. Lucas, E. Kartheuser, and R. G. Badro, Phys. Rev. B **2**, 2488 (1970).
[28] T. L. Ferrell and P. M. Echenique, Phys. Rev. Lett. **55**, 1526 (1985).
[29] C. Denton, J. L. Gervasoni, R. O. Barrachina, and N. R. Arista, Phys. Rev. A **57**, 4498 (1998).
[30] M. Abramowitz and I. A. Stegun, *Handbook of Mathematical Functions* (Dover, New York, 1972).
[31] D. Pines, *Elementary Excitations in Solids* (Benjamin, New York, 1964).
[32] D. L. Mills, Phys. Rev. B **15**, 763 (1977), and references therein.
[33] A. A. Lucas, L. Henrard, and Ph. Lambin, Phys. Rev. B **49**, 2888 (1994).